miRNA profiling of primate cervicovaginal lavage and extracellular vesicles reveals miR-186-5p as a potential retroviral restriction factor in macrophages

Zezhou Zhao[1,#], Dillon C. Muth[1,3,#], Kathleen Mulka[1], Bonita H. Powell[1], Grace V. Hancock[1,&], Zhaohao Liao[1], Kelly A. Metcalf Pate[1], Kenneth W. Witwer[1,2,3,*]

[1]Department of Molecular and Comparative Pathobiology, [2]Department of Neurology, and [3]Cellular and Molecular Medicine Program, The Johns Hopkins University School of Medicine, Baltimore, MD, USA.

[#] These authors contributed equally to this work

[&]Currently at Molecular Biology Institute, University of California, Los Angeles, Los Angeles, California, USA.

*Address correspondence to:

Kenneth W. Witwer, PhD

733 N. Broadway

Miller Research Building 829

Baltimore, MD 21205

Phone: 1-410-955-9770

Fax: 1-410-955-9823

Email: kwitwer1@jhmi.edu

Keywords: extracellular vesicle, exosome, microvesicle, microRNA, biomarker, HIV-1, cervicovaginal lavage, SIV, restriction factor

Abstract

Introduction: The goal of this study was to characterize extracellular vesicles (EVs) and miRNA profiles of primate cervicovaginal lavage (CVL) during the menstrual cycle and simian immunodeficiency virus (SIV) infection, and to determine if CVL-associated miRNAs might influence replication of retroviruses.

Methods: CVL and peripheral blood were collected for five weeks from two uninfected and four SIV-infected macaques. EVs were enriched by stepped ultracentrifugation and characterized by population-level and single vesicle analyses. miRNA profiles were assessed with a medium-throughput stem-loop/hydrolysis probe qPCR platform and validated by targeted qPCR assays. Influence of miR-186-5p ("miR-186") on HIV protein and RNA production was monitored in monocyte-derived macrophages.

Results: Although menstrual hormone cycling was abnormal in infected subjects, EV concentration increased with progesterone in uninfected subjects. miRNAs were present predominantly in the EV-depleted supernatant fraction of CVL. Few changes in miRNA levels correlated with the menstrual cycle or SIV infection. miR-186, depleted in retroviral infection, was investigated for a possible role in controlling retroviral infection. miR-186 inhibited HIV production when transfected into monocyte-derived macrophages.

Conclusions: We report profiles of a targeted set of miRNAs in CVL fractions. The menstrual cycle may affect quantity of EVs recovered from CVL, but has only minor effects on abundance of the miRNAs we examined. miR-186 decline appears to be associated with SIV infection, and miR-186 inhibits HIV replication in macrophages in vitro. Further studies are required to characterize the role of EVs and small RNAs as biomarkers of disease in the reproductive tract.

Introduction

The cervicovaginal canal is a potential source of biological markers in forensics investigations [1–4] and reproductive tract cancers [5] and infections [6]. Cervicovaginal secretions may be collected by swab, tampon, or other methods, or secretion components may be liberated by a buffered wash solution and collected as cervicovaginal lavage (CVL). Beyond utility as biomarkers, constituents of cervicovaginal secretions including proteins [7] and certain microbes [8] may have protective roles, for example in wound healing and against HIV-1 infection [9–16]. Secreted components may also change quantitatively or qualitatively during the menstrual cycle [17].

Compared with secreted proteins and the microbiome, several components of cervicovaginal fluids are less well understood, including extracellular RNAs (exRNAs) and their carriers, such as extracellular vesicles (EVs) and ribonucleoprotein complexes (exRNPs). EVs are potential regulators of cell behavior in paracrine and endocrine fashion due to their reported abilities to transfer proteins, nucleic acids, sugars, and lipids between cells [18]. EVs comprise a wide array of double-leaflet membrane extracellular particles, including exosomes and microvesicles [19], and range in diameter from 30 nm to well over one micron (large oncosomes) [20]. EV macromolecular composition tends to reflect, but is not necessarily identical to, that of the cell of origin [21]. EVs have been isolated from most cells, as well as biological fluids [18, 22], including cervicovaginal secretions of humans [23] and rhesus macaques [24].

microRNAs (miRNAs) are one of the most studied classes of exRNA. These noncoding RNAs average 22 nucleotides in length and, in some cases, fine-tune the expression of target transcripts [25, 26]. Released from cells by several routes, miRNAs are among the most frequently examined biomarker candidates in biofluids and are reported to be transmitted via EVs. miRNAs

are found not only in EVs, but also in free Argonaute-containing protein complexes; the latter may outnumber the former, at least in blood [27, 28]. miRNAs are also highly conserved [26], and abundant species typically have 100% identity in humans and nonhuman primates [29]. (For this reason, we will refer to hsa- (Homo sapiens) and mml- (*Macaca mulatta*) miRNAs without the species designation unless otherwise warranted by sequence disparity.) While miRNAs have been profiled in cervicovaginal secretions and menstrual blood, mostly in the forensics setting [4, 30, 31], their associations with EV and exRNP fractions require further study. A recent publication reported that EVs from healthy vaginal secretions inhibited HIV-1 infection [23]. Another report found that CVL EVs (termed “exosomes”) were present at higher concentrations in cervical cancer, and that two miRNAs were also upregulated [5]. Our group described a reduction of CVL EVs in a severe endometriosis case compared with reproductively healthy primates [24]. However, our study, along with others, was limited by the absence of molecular profiling of EV cargo [24].

Here, we performed targeted miRNA profiling of EV-enriched and -depleted fractions of CVL and vaginal secretions collected from healthy and retrovirus-infected rhesus macaques. We queried how CVL EVs and miRNAs are affected by the menstrual cycle, an important potential confounder of biomarker studies. Similarly, we assessed possible associations with simian immunodeficiency virus (SIV) infection. We report an association of miR-186 levels with SIV infection and find that this miRNA also appears to act in an antiretroviral fashion in HIV infection of macrophages. These studies provide baseline information for easily accessed CVL markers including EVs and miRNAs that may become useful tools in the clinic.

METHODS

Sample Collection

CVL and whole blood samples were collected weekly for five weeks from two uninfected (control) and four SIVmac251-infected (infected) rhesus macaques (*Macaca mulatta*) as previously described [24]. All macaques were negative for simian T-cell leukemia virus and simian type D retrovirus and were inoculated intravenously. Animals were sedated with ketamine at a dose of 7-10 mg/kg prior to all procedures. CVL was performed by washing the cervicovaginal cavity with 3 mL of phosphate buffered saline (PBS, Thermo Fisher Scientific, Waltham, MA, USA) directed into the cervicovaginal canal and re-aspirated using the same syringe. Materials and procedures for sample collection are depicted in Supplemental Figure 1. Volumes of CVL yield across collection dates were documented in Supplemental Table 1. Whole blood (3 mL) was collected by venipuncture into syringes containing acid citrate dextrose solution (ACD) (Sigma Aldrich, St. Louis, MO, USA).

Study Approvals

All animal studies were approved by the Johns Hopkins University Institutional Animal Care and Use Committee (IACUC) and conducted in accordance with the Weatherall Report, the Guide for the Care and Use of Laboratory Animals, and the USDA Animal Welfare Act.

Sample Processing

Sample processing began within a maximum of 60 minutes of collection and utilized serial centrifugation steps to enrich EVs as described previously [32], based on a standard EV isolation protocol [33]. Specifically, fluids were centrifuged: (1) 1,000 × *g* for 15mins at 4°C in a tabletop centrifuge; (2) 10,000 × *g* for 20 mins at 4°C; and (3) 110,000 × *g* for 2 hours at 4°C with a Sorvall Discovery SE ultracentrifuge (Thermo Fisher Scientific) with an AH-650 rotor (k factor: 53.0) (Supplemental Figure 1B). Following each centrifugation step, most supernatant was removed, taking care not to disturb the pellet. After each step, supernatant was set aside for nanoparticle tracking analysis (NTA; 200 µL), and RNA isolation (200 µL) following the second and third steps. The pellet was resuspended in 400 µL of PBS after each centrifugation step. After the final step, the remaining ultracentrifuged supernatant was concentrated to approximately 220 µL using Amicon Ultra-2 10 kDa molecular weight cutoff filters (Merck KGaA, Darmstadt, Germany). 200 µL of the concentrate was used for RNA isolation and the remainder was retained for NTA. All samples reserved for RNA isolation were mixed with 62.6 µL of RNA isolation buffer (Exiqon, Vedbaek, Denmark) containing three micrograms of glycogen and 5 pg of synthetic cel-miR-39 as previously described [34]. Processed samples were analyzed immediately or frozen at -80°C until further use.

For plasma, whole blood was centrifuged at 800 × *g* for 10 mins at 25°C. Supernatant was centrifuged twice at 2,500 × *g* for 10 mins at 25°C. The resulting platelet-poor plasma was aliquoted and frozen at -80°C.

Hormone Analysis

Levels of progesterone (P4) and estradiol-17b (E2) were measured in plasma samples shipped overnight on dry ice to the Endocrine Technology and Support Core Lab at the Oregon National Primate Research Center, Oregon Health and Science University.

Nanoparticle Tracking Analysis

Extracellular particle concentration was determined using a NanoSight NS500 NTA system (Malvern, Worcestershire, UK). Cervicovaginal lavage samples were diluted as needed and specified in Supplemental Table 2 to ensure optimal NTA analysis. At least five 20-second videos were recorded for each sample at a camera setting of 12. Data were analyzed at a detection threshold of two using NanoSight software version 3.0.

Western Blot

Western blot was used to detect the presence of EV protein markers and the absence of calnexin (endoplasmic reticulum marker) in CVL and enriched CVL EVs. Because of low quantities, both CVL and enriched EVs were pooled as indicated in Supplemental Table 3. 20 µL of pooled samples were lysed with 5 µL 1:1 mixture of RIPA buffer (Cell Signaling Technology, Danvers, MA. Cat #: 9806S) and protease inhibitor (Santa Cruz Biotechnology, Dallas, TX. Cat #: sc29131). 8 µL of Laemmli 4X sample buffer (BioRad, Hercules, CA. Cat #:161-0747 Lot #: 64077737) was added per sample, and 30 µL of each was loaded into a Criterion TGX 10% gel (BioRad, Hercules, CA. Cat #: 5671034 Lot #: 64115589) after 5 mins of 95ºC incubation. The gel was electrophoresed by application of 100V for 100 mins. The proteins were then transferred to a PVDF membrane (BioRad, Hercules, CA), which was blocked with 5% milk (BioRad,

Hercules, CA. Cat #: 1706404. Lot #: 64047053) in PBS+0.1%Tween®20 (Sigma-Aldrich, St. Louis, MO Cat #: 274348 Lot #: MKBF5463V) for 1 hour. The membrane was subsequently incubated with mouse anti-human CD63 (BD Biosciences, San Jose, CA Cat #: 556019 Lot #: 6355939) and mouse monoclonal IgG_2b CD81 (Santa Cruz Biotechnology, Dallas, TX Cat #: 166029 Lot #: L1015) primary antibodies, at a concentration of 0.5 µg/mL for 1 h. After washing the membrane, it was incubated with a goat anti-mouse IgG-HRP secondary antibody (Santa Cruz Biotechnology, Dallas, TX Cat #: sc-2005 Lot #: B1616) at a 1:10,000 dilution for 1 h. The membrane was then incubated with a 1:1 mixture of SuperSignal West Pico Stable Peroxide solution and Luminol Enhancer solution (Thermo Scientific, Rockford, IL Cat #: 34080 Lot #: SD246944) for 5 min. The membrane was visualized on chemiluminescence film (Denville Scientific, Holliston, MA Cat #: E3018 Lot #:79608091) for up to 150 seconds. The second blot was done in a reducing environment using 10mM DTT (Promega, Madison, WI Cat #: P1171 Lot #: 0000198991). Same procedures were followed with rabbit anti-human TSG101 (Cat #: ab125011 Lot #:GR180132-14), rabbit anti-syntenin (Abcam, Cambridge, MA Cat #: ab133267 Lot #: GR89146-10), and rabbit anti-calnexin (Abcam, Cambridge, MA Cat #: ab22595 Lot #:GR243392-3) primary antibodies. Subsequent incubation with goat anti-rabbit IgG-HRP secondary antibody (Abcam, Cambridge, MA Cat #: sc-2204 Lot #: B2216). All antibodies were used at the same concentration as the first blot. Film was exposed to the membrane for up to 8 mins for visualization.

Electron Microscopy

Gold grids were floated on 2% paraformaldehyde-fixed CVL–derived samples for two minutes, then negatively stained with uranyl acetate for 22 seconds. Grids were observed with a Hitachi

7600 transmission electron microscope in the Johns Hopkins Institute for Basic Biomedical Sciences Microscope Facility.

Total RNA Isolation and Quality Control

RNA isolation work flow is shown in Supplemental Figure 1C. RNA lysis buffer was added into each sample as described above prior to freezing (-80 °C). Total RNA was isolated from thawed samples using the miRCURY RNA Isolation Kit-Biofluids (Exiqon) per manufacturer's protocol with minor modifications as previously described (10). Total RNA was eluted with 50 µL RNase-free water and stored at -80°C. As quality control, expression levels of several small RNAs including snRNA U6, miR-16-5p, miR-223-3p, and the spiked-in synthetic cel-miR-39 were assessed by TaqMan miRNA assays (Applied Biosystems/ Life Technologies, Carlsbad, California, USA) [35].

miRNA Profiling by TaqMan Low-Density Array

A custom 48-feature TaqMan low-density array (TLDA) (11) was ordered from Thermo Fisher, with features chosen based on results of a human CVL pilot study (G. Hancock and K.W. Witwer, unpublished data). Stem-loop primer reverse transcription and pre-amplification steps were conducted using the manufacturer's reagents as previously described [36] but with 14 cycles of pre-amplification. Real time quantitative PCR was performed with a QuantStudio 12K instrument (Johns Hopkins University DNA Analysis Facility). Data were collected using SDS software and Cq values extracted with Expression Suite v1.0.4 (Thermo Fisher Scientific,

Waltham, MA USA). Raw Cq values were adjusted by a factor determined from the geometric mean of 10 relatively invariant miRNAs. The selection process for these invariant miRNAs was to 1) rank miRNAs by coefficient of variation; 2) remove miRNAs with high average Cq (>30), non-miRNAs, and those with low amplification score; 3) select the lowest-CV member of miRNA families (e.g., the 17/92 clusters); and 4) pick the top 10 remaining candidates by CV: let-7b-5p, -miR-21-5p , -27a-3p, -28-3p, -29a-3p, -30b-5p, -92a-3p, -197-3p, -200c-3p, and -320a-3p.

Individual RT-qPCR Assays

Individual TaqMan miRNA qPCR assays were performed as previously described [36] for miRs-19a-3p (Thermo Fisher Assay ID #000395), -186-5p (Thermo Fisher Assay ID #002285), -451a-5p (Thermo Fisher Assay ID #001105) , -200c-3p (Thermo Fisher Assay ID #002300), -222-3p (Thermo Fisher Assay ID #002276), -193b-3p (Thermo Fisher Assay ID #002367), -181a-5p (Thermo Fisher Assay ID #000480), and -125b-5p (Thermo Fisher Assay ID #00449). We also measured miR-375-3p (Thermo Fisher Assay ID #00564), which was not included on the array. Data were adjusted to Cqs of miR-16-5p and miR-19a-3p, but conclusions were robust to different normalization methods.

Blood Cell Isolation and Monocyte-Derived Macrophage Culture

Total PBMCs were obtained from freshly drawn blood from human donors under a Johns Hopkins University School of Medicine IRB-approved protocol (JHU IRB #CR00011400). Blood was mixed with 10% Acid Citrate Dextrose (ACD) (Sigma Aldrich, St. Louis, MO Cat #:

C3821 Lot #: SLBQ6570V) with gentle mixing by inversion. Within 15 minutes of draw, blood was diluted with equal volume of PBS+ 2% FBS, gently layered onto room temperature Ficoll (Biosciences AB, Uppsala, Sweden Cat #:17-1440-03 Lot #: 10253776) in Sepmate-50 tubes (STEMCELL Technologies, Vancouver, BC, Canada Cat #: 15450 Lot #: 06102016) and centrifuged for 10 minutes at 1200 × *g*. Plasma and PBMC fractions were removed, washed in PBS+ 2% FBS, and pelleted at 300 × *g* for 8 minutes. Pellets from 5 tubes were combined by resuspension in 10 mL RBC lysis buffer (4.15 g NH_4Cl, 0.5 g $KHCO_3$, 0.15 g EDTA in 450 mL H_2O; pH adjusted to 7.2–7.3; volume adjusted to 500 mL and filter-sterilized); total volume was brought to 40 mL with RBC lysis buffer. After incubation at 37 °C for 5 mins, the suspension was centrifuged at 400 × *g* for 6 mins at room temperature. The cell pellet was resuspended in Macrophage Differentiation Medium with 20% FBS (MDM20) to a final concentration of 2×10^6 cells/mL. PBMCs were plated at 4×10^6 cells per well in 12-well plates and cultured in MDM20 for 7 days. One half of the total volume of medium was replaced on day 3. On day 7, cells were washed 3 times with PBS to remove non-adherent cells. The medium was replaced with Macrophage Differentiation Medium with 10% serum (MDM10) and cultured overnight prior to transfection.

miRNA Mimic Transfection

Differentiated macrophages were transfected with 50 nM miRNA-186-5p using Lipofectamine 2000 (Invitrogen/Life Technologies, Carlsbad, CA Cat #: 11668-019 Lot #:1467572) diluted in OptiMEM Reduced Serum Medium (Gibco, Grand Island, NY Cat #: 31985-070 Lot #: 1762285). Controls included mock transfections and transfection of 50 nM siRNA oligo labeled with Alexa Fluor 555 (Invitrogen, Fredrick, MD Cat #: 14750-100 Lot #: 1863892). Plates were

incubated for 6 hours at 37 °C. After incubation, successful transfection was confirmed by examining uptake of labeled siRNA with an Eclipse TE200 inverted microscope (Nikon Instruments, Melville, NY). Transfection medium was removed. The plates were washed with PBS and refed with 2 mL fresh MDM10 medium.

HIV Infection

HIV-1 BaL stocks were generated from infected PM1 T-lymphocytic cells and stored at −80□°C. 24 hours after mimic or mock transfections, macrophages were infected with HIV BaL and incubated overnight (stock, 80 µg p24/mL, diluted to 200 ng p24/mL). At days 3, 6, and 9 post-infection, 500 µL supernatant was collected for p24 release assays and cells were lysed with 600 µL mirVana lysis buffer for subsequent RNA isolation and analysis.

HIV p24 Antigen ELISA

Supernatant samples were lysed with Triton-X at a final concentration of 1%. The DuPont HIV-1 p24 Core Profile ELISA kit (Perkin Elmer, Waltham, MA Cat #: NEK050B001KT Lot #: 990-17041) was used per manufacturer's instructions to measure p24 concentration based on the provided standard.

Total RNA Isolation

Total RNA was isolated using the mirVana miRNA Isolation Kit per manufacturer's protocol (Ambion, Vilnius, Lithuania Cat #: AM1560 Lot #: 1211082). Note that this procedure yields total RNA, not just small RNAs. After elution with 100 µL RNase-free water, nucleic acid

concentration was measured using a NanoDrop 1000 spectrophotometer (Thermo Fisher Scientific, Wilmington, DE). RNA isolates were stored at -80 °C.

HIV Gag RNA RT-qPCR

Real-time one-step reverse transcription quantitative PCR was performed with the QuantiTect Virus Kit (Qiagen, Foster City, CA Cat #:211011 Lot #: 154030803). Each 25 µl reaction mixture contained 15 µl of master mix containing HIV-1 RNA standard, 100 µM of FAM dye and IBFQ quencher labeled Gag probe (5' ATT ATC AGA AGG AGC CAC CCC ACA AGA 3'), 600 nM each of Gag1 forward primer (5'TCA GCC CAG AAG TAA TAC CCA TGT 3') and Gag2 reverse primer (5' CAC TGT GTT TAG CAT GGT GTT T 3'), nuclease-free water, and QuantiTect Virus RT mix, and 10 µL serial-diluted standard or template RNA. No-template control and no reverse transcriptase controls were included. Linear standard curve was generated by plotting the log copy number versus the quantification cycle (C_q) value. Log-transformed Gag copy number was calculated based on the standard curve.

Macrophage Viability Assessment by MTT Cell Proliferation Assay

5 mg 3-(4,5-Dimethylthiazol-2-yl)-2,5- diphenyltetrazolium bromide (MTT) (Vybrant MTT cell proliferation assay kit, Invitrogen, Eugene, OR Cat #: V13154 Lot #: 1897699) was dissolved in 1mL of PBS and incubated in the dark for 20 mins. Dissolved MTT was then diluted in 12 mL of phenol red-free MDM10 medium. Macrophages in 12 well plates were washed with 2 mL PBS. 1 mL of MTT/MDM10 medium was added to each well and incubated at 37 °C for 45 mins. 12 mL of 0.01N hydrochloric acid was added to dissolve SDS, and 1 mL acidified SDS solution was added to each well and mixed thoroughly until all formazan crystals were dissolved. Formazan

quantification was performed using an iMark microplate absorbance reader (BioRad, Hercules, CA) with a 570 nm test wavelength. Data were expressed as mean absorbance value (OD) of duplicate samples plus standard error of the mean.

Data analysis

Data processing and analysis were conducted using tools from Microsoft Excel (geometric mean normalization), Apple Numbers, GraphPad Prism, the MultiExperiment Viewer, and R/BioConductor packages including pheatmap (http://CRAN.R-project.org/package=pheatmap; quantile normalization, Euclidean distance, self-organizing maps, self-organizing tree algorithms, k-means clustering). Figures and tables were prepared using R Studio, Microsoft Excel and Word, Apple Numbers and Keynote, GraphPad Prism, and Adobe Photoshop.

Data Availability and Rigor and Reproducibility

Array data have been deposited with the Gene Expression Omnibus (GEO) [37] as GSE107856. Data in other formats are available upon request. To the extent that sample quantities would allow, the MISEV2014 recommendations for EV studies were followed [38, 39], and the EV experiments have been registered with the EV-TRACK knowledgebase [40] with preliminary EV-TRACK code XL5296IL.

RESULTS

Abnormal menstrual cycle of SIV-infected macaques and ovulation-associated changes in levels of CVL EV-enriched particles

Plasma and CVL were collected from two control and four SIV-infected macaques over the course of five weeks (Supplemental Figure 1). Abnormal cycling was observed for infected subjects (K. Mulka, et al, manuscript in preparation). By nanoparticle tracking analysis, CVL EV concentration increased during ovulation (Figure 1A). Transmission electron microscopy was performed for representative fractions of CVL, revealing bacteria and associated particles in the 1,000 × *g* pellet (Figure 1B). The 100,000 x g pellet included apparent EVs up to 200 nm in diameter (Figure 1C). EV markers (shown: CD63 and CD81) were confirmed by Western blot in samples from control and infected subjects (Figure 1D). Calnexin was found only in tissue samples (Figure 1E). Interestingly, neither TSG101 nor syntenin (considered to be luminal EV proteins) could be detected in the EV-enriched fractions of CVL (Figure 1E), potentially indicating a predominance of surface-released EVs over endosomal-origin exosomes in these preparations.

Extracellular miRNAs of the cervicovaginal compartment

Based upon preliminary findings from a study of human CVL (Hancock and Witwer, unpublished data), we designed a custom TaqMan low-density array (TLDA) to measure 47 miRNAs expected to be present in CVL, along with the snRNA U6. CVL from all subjects and at all time points was fractionated by stepped centrifugation to yield a 10,000 x g pellet (10K pellet or p10), a 100,000 x g pellet (UC pellet or p100), and 100,000 x g supernatant (UC

supernatant or S100). Total RNA from all fractions was profiled by TLDA. Raw (Figure 2A), quantile normalized (Figure 2B), and geometric mean-adjusted Cq values (Figure 2C) were subjected to unsupervised hierarchical clustering. This clustering did not reveal broad miRNA profile differences associated with sample collection time, menstruation, or SIV infection.

Distribution of miRNAs across CVL fractions

Across the three examined CVL fractions (p10, p100, S100), the ten most abundant miRNAs (lowest Cq values) were miRs-223-3p, -203a-3p, -24-3p, -150-5p, -146a-5p, -21-5p, -222-3p, -92a-3p, -17-5p, and -16-5p. The average normalized Cq value for each miRNA was greater (i.e., lower abundance) in the p100 than in the S100 fraction (Figure 3A and inset), and indeed in p10 and p100 combined (Figure 3B), suggesting that most miRNA in CVL, as in various body fluids, is found outside the EV-enriched fractions. Considering all fractions, the differences between the EV-enriched and EV-depleted fractions were significant even after Bonferroni correction for all features except U6, miR-191-5p, and miR-451a-5p. On average, the S100 fraction contained 86.5% of the total miRNA from these three fractions. In the p10 fraction, the average miRNA was detected at 10.5% its level in the S100 fraction (SD=5.7%). miR-34a-5p had the lowest (5.9%) and miR-28-3p the highest (33.7%) abundance compared with S100. In the p100 fraction, miRNAs were on average 5.6% (SD=2.4%) as abundant as in S100. The least represented in p100 was miR-27a-3p (2.3%), and the best represented was again miR-28-3p (13.4%). miRNA rank was significantly correlated across fractions, despite minor differences in order (Figure 3C).

qPCR validation

Individual stem loop RT/hydrolysis probe qPCR assays were used to verify TLDA results for miRs-19a-3p, -186-5p, -451a-5p, -200c-3p, -222-3p, -193b-3p, -181a-5p, and -125b-5p. miR-375-3p (not included on the array), was also measured because of a reported association with goblet cells (12). Results of qPCR assays, adjusted by miR-16-5p for each sample, are shown in Figure 4A. Figure 4B compares miRNA ranks (1-11) by TLDA and individual qPCR, which are generally in concordance. Note that expression of red blood cell miRNA miR-451a-5p was low, suggesting minimal contamination from blood for most samples.

miRNAs and retroviral infection status

An association of miRNA abundance with infection status could yield novel biomarkers as well as clues to roles of miRNA in modulating infection. However, the small number of subjects in our study was a challenge. Nevertheless, by considering all subjects and time points together for both infected and uninfected subjects, microarray data suggested a slightly reduced abundance of miRs-186-5p, -222-3p, and -200c-3p in infected samples, while qPCR revealed differential abundance of miRs-186-5p, -375-3p, and -125b-5p. (Figure 5). miR-186-5p was thus identified by both techniques as potentially associated with retroviral infection.

miR-186-5p inhibits HIV p24 release by monocyte-derived macrophages. To assess a possible influence of miR-186-5p ("miR-186") on retroviral replication, we introduced miR-186 mimic or control RNAs into monocyte-derived macrophages 24 hours before infection or not with HIV. At days 3, 6, and 9 post-infection (dpi), we measured HIV release (capsid p24 protein in culture supernatant) and transcription (cellular Gag mRNA copy number). By p24 release,

robust infection was observed by 3 dpi, and p24 counts increased by two-fold or more by 9 dpi (Figure 6A) for multiple replicate experiments with cells from three donors. Compared with infected, untreated controls, mock-transfected cells (not shown), and cells transfected with a negative control RNA (labeled with a fluorophore to assess transfection efficiency), miR-186 transfection was associated with a significant decline of released p24 at all time points (ANOVA with Bonferroni correction) (Figure 6B-D). The negative control condition showed a suppressive trend that reached nominal significance at 9 dpi. However, miR-186-associated suppression was significantly greater at all time points.

No consistent effect of miR-186 on HIV RNA abundance

Using a gag qPCR/standard curve, we quantitated full-length HIV-1 transcript in cells from three donors. In cells from only one of three donors were fewer HIV-1 copies associated with miR-186 mimic transfection (Figure 7). Overall, there was no statistically significant difference in HIV RNA between the conditions.

DISCUSSION

Cervicovaginal lavage and CVL EVs and exRNPs, like EVs in the uterus [41, 42], may offer information about the health of the reproductive tract as well as clues about factors that facilitate or block transmission of infectious agents. Proteomic analyses of human [43] and rhesus macaque [44] CVL have suggested a core proteome and a highly variable proteome that responds to changes in pregnancy status, menstruation, infection, and other stressors. However, exRNA and extracellular vesicle profiles are less understood in this compartment. Thus, the major finding of this study is further characterization of CVL fluid of primates, including extracellular vesicle and miRNA profiles. EVs could be liberated from vaginal secretions by lavage, and these EVs could be concentrated using a standard stepped centrifugation procedure, with enrichment of positive (membrane-associated) markers and apparent absence of a cellular negative control. Furthermore, both EV-replete and EV-depleted fractions of CVL contained abundant miRNA.

As reported for other biological fluids [27, 45], miRNA concentration was highest in the EV-depleted CVL fractions, not in EV-enriched ultracentrifuged pellets, consistent with packaging of most extracellular miRNA into exRNPs; the function, if any, of extracellular miRNAs in the cervicovaginal tract of healthy individuals remains to be determined. We observed minimal differences in extracellular miRNA profiles between SIV-infected and uninfected subjects or, most surprisingly, during the course of the menstrual cycle, suggesting a certain stability of extracellular miRNA in the compartment. Correlation of miRNA concentrations in EV-depleted and -replete fractions was also apparent. Based on relative abundance, miRNAs in EVs and exRNPs of CVL are likely derived from epithelial cells (including goblet cells), and cells of the immune system (as suggested, e.g., by myeloid-enriched miR-223 and lymphocyte-enriched miR-150) [46]. Of the most abundant miRNAs we identified, many have been ascribed tumor-

409 suppressive roles in various types of cancer (14–19). Also, miR-223 and miR-150 have been
410 described as "anti-HIV" miRNAs [53] among a variety of reported antiretroviral sRNAs, both
411 host and viral [54–59]. Given their relative abundance in the vaginal tract, a common site for
412 HIV infection, these miRNAs may contribute to antiviral defenses.

413 Along these lines, a second major finding of this study is a possible role for miR-186 in anti-
414 retroviral defense. In contrast with an early report of direct binding of host miRNAs to retroviral
415 transcripts and subsequent suppression [53], it now appears that this mechanism of suppression is
416 relatively uncommon [60], and that anti-HIV miRNAs may exert effects through control of host
417 genes instead [e.g., [61]]. Our data also support the conclusion that reduction of HIV RNA levels
418 is not the main mechanism for miR-186-mediated suppression of HIV release.

419 We would like to emphasize several weaknesses of the study and opportunity for future research:

420 1) We used stepped ultracentrifugation without density gradients because of the small sample
421 volumes available. Although stepped ultracentrifugation remains a widely used method for EV
422 enrichment [33, 62], subsequent gradients or alternative isolation methods could be attempted
423 with larger volume samples to increase purity in future. Possibly, our study overestimates the
424 abundance of miRNAs in CVL EVs, and differential packaging into EVs and exRNPs is masked
425 by contamination of our EV preps with exRNPs.

426 2) Our qPCR array approach and focus on miRNAs leaves room for additional work. While we
427 are confident that our array captured most of the abundant miRNAs in CVL, sequencing short
428 and longer RNAs could reveal additional markers.

429 3) The small number of subjects and the absence of obvious menstrual cycle in infected subjects
430 precludes strong conclusions about EV or miRNA associations with either infection or the

menstrual cycle. For example, we did not observe the expected increase in miR-451a or other red blood cell-specific miRNAs during menstruation. However, since only two animals showed evidence of cycling, experiments with more subjects and larger sample volumes are needed.

4) Our previous criticisms of miRNA functional studies [63] also apply to our work here. Additional work is needed to prove that miR-186 can regulate retroviral release at endogenous levels, that it is present in active RNPs [64], its interactions with host targets, and a mechanism for viral suppression. Finally, it is possible, but must be demonstrated, that miR-186 acts in a paracrine fashion via EV or exRNP shuttles.

5) We have investigated the effects of miR-186 only in monocyte-derived macrophages. We chose to begin with this cell type because of the abundance of miR-223 and the known role of macrophages in the epithelium. Other cell types should also be investigated.

Overall, the results presented here support further development of CVL and its constituents as a window into the health of the cervicovaginal compartment.

ACKNOWLEDGMENTS

The authors thank Robert Adams, Lauren Ostrenga, and Sarah Beck for contributions to these studies. The authors gratefully acknowledge the Oregon National Primate Research Center and David Erikson for hormone analyses and endocrinology advice and thank Barbara Smith of the JHU IBBS Microscope Facility for expert assistance with electron microscopy. Amanda Steele provided paid assistance with editing and organizing an early version of the manuscript.

AUTHOR CONTRIBUTIONS

All authors have accepted responsibility for the entire content of this submitted manuscript and approved submission. ZZ and DM performed experiments and analyses and contributed to writing the paper; KM and DM collected and processed samples; KAMP provided clinical assistance; ZL, BHP, and GVH performed experiments; KWW planned and directed the studies, conducted analyses, and wrote and edited the manuscript.

FUNDING

This work was supported in part by the US National Institutes of Health through R01 DA040385 (to KWW); by the Johns Hopkins University Center for AIDS Research, an NIH funded program (P30AI094189; pilot grant to KWW and summer research fellowship to ZZ); and by the National Center for Research Resources and the Office of Research Infrastructure Programs (ORIP) and the National Institutes of Health (P40 OD013117). DM and KM received support through NIH T32 OD011089.

COMPETING INTERESTS

The authors have no competing interests to declare. The funding organization(s) played no role in the study design; in the collection, analysis, and interpretation of the data; in the writing of the report; or in the decision to submit the report for publication.

REFERENCES

1. Hanson EK, Ballantyne J (2013) Highly specific mRNA biomarkers for the identification of vaginal secretions in sexual assault investigations. Sci Justice 53:14–22. doi: 10.1016/j.scijus.2012.03.007

2. Jakubowska J, MacIejewska A, Pawłowski R, Bielawski KP (2013) MRNA profiling for vaginal fluid and menstrual blood identification. Forensic Sci Int Genet 7:272–278. doi: 10.1016/j.fsigen.2012.11.005

3. Park JL, Kwon OH, Kim JH, et al (2014) Identification of body fluid-specific DNA methylation markers for use in forensic science. Forensic Sci Int Genet 13:147–153. doi: 10.1016/j.fsigen.2014.07.011

4. Hanson EK, Lubenow H, Ballantyne J (2009) Identification of forensically relevant body fluids using a panel of differentially expressed microRNAs. Anal Biochem 387:303–314. doi: 10.1016/j.ab.2009.01.037S0003-2697(09)00065-7 [pii]

5. Liu J, Sun H, Wang X, et al (2014) Increased Exosomal MicroRNA-21 and MicroRNA-146a Levels in the Cervicovaginal Lavage Specimens of Patients with Cervical Cancer. Int J Mol Sci Int J Mol Sci 15:758–773. doi: 10.3390/ijms15010758

6. Gravett MG, Thomas A, Schneider KA, et al (2007) Proteomic Analysis of Cervical−Vaginal Fluid: Identification of Novel Biomarkers for Detection of Intra-amniotic Infection. J Proteome Res 6:89–96. doi: 10.1021/pr060149v

7. Burgener A, Boutilier J, Wachihi C, et al (2008) Identification of differentially expressed proteins in the cervical mucosa of HIV-1-resistant sex workers. J Proteome Res 7:4446–

4454. doi: 10.1021/pr800406r

8. Zevin AS, Xie IY, Birse K, et al (2016) Microbiome Composition and Function Drives Wound-Healing Impairment in the Female Genital Tract. PLoS Pathog 12:e1005889. doi: 10.1371/journal.ppat.1005889

9. Boggiano C, Littman DR (2007) HIV's Vagina Travelogue. Immunity 26:145–147. doi: 10.1016/j.immuni.2007.02.001

10. Patel M V., Ghosh M, Fahey J V., et al (2014) Innate Immunity in the Vagina (Part II): Anti-HIV Activity and Antiviral Content of Human Vaginal Secretions. Am J Reprod Immunol 72:22–33. doi: 10.1111/aji.12218

11. Benki S, Mostad SB, Richardson BA, et al (2008) Increased levels of HIV-1-infected cells in endocervical secretions after the luteinizing hormone surge. J Acquir Immune Defic Syndr 47:529–34. doi: 10.1097/QAI.0b013e318165b952

12. Zara F, Nappi RE, Brerra R, et al (2004) Markers of local immunity in cervico-vaginal secretions of HIV infected women: implications for HIV shedding. Sex Transm Infect 80:108–112. doi: 10.1136/sti.2003.005157

13. Gardella B, Roccio M, Maccabruni A, et al (2011) HIV shedding in cervico-vaginal secretions in pregnant women. Curr HIV Res 9:313–20. doi: Abs: CHIVR-162 [pii]

14. Seaton KE, Ballweber L, Lan A, et al (2014) HIV-1 specific IgA detected in vaginal secretions of HIV uninfected women participating in a microbicide trial in Southern Africa are primarily directed toward gp120 and gp140 specificities. PLoS One. doi: 10.1371/journal.pone.0101863

15. Ghosh M, Fahey J V., Shen Z, et al (2010) Anti-HIV activity in cervical-vaginal secretions from HIV-Positive and -Negative women correlate with innate antimicrobial levels and IgG antibodies. PLoS One. doi: 10.1371/journal.pone.0011366

16. Clemetson DB, Moss GB, Willerford DM, et al (1993) Detection of HIV DNA in cervical and vaginal secretions. Prevalence and correlates among women in Nairobi, Kenya. Jama 269:2860–2864. doi: 10.1016/0020-7292(94)90090-6

17. Rahman S, Rabbani R, Wachihi C, et al (2013) Mucosal serpin A1 and A3 levels in HIV highly exposed sero-negative women are affected by the menstrual cycle and hormonal contraceptives but are independent of epidemiological confounders. Am J Reprod Immunol 69:64–72. doi: 10.1111/aji.12014

18. Yáñez-Mó M, Siljander PR-M, Andreu Z, et al (2015) Biological properties of extracellular vesicles and their physiological functions. J Extracell vesicles 4:27066.

19. Gould SJ, Raposo G (2013) As we wait: coping with an imperfect nomenclature for extracellular vesicles. J Extracell Vesicles. doi: 10.3402/jev.v2i0.2038920389 [pii]

20. Meehan B, Rak J, Di Vizio D (2016) Oncosomes - large and small: what are they, where they came from? J Extracell vesicles 5:33109.

21. György B, Hung ME, Breakefield XO, Leonard JN (2015) Therapeutic applications of extracellular vesicles: clinical promise and open questions. Annu Rev Pharmacol Toxicol 55:439–64. doi: 10.1146/annurev-pharmtox-010814-124630

22. Witwer KW, Buzás EI, Bemis LT, et al (2013) Standardization of sample collection, isolation and analysis methods in extracellular vesicle research. J Extracell vesicles 2:1–25.

537 doi: 10.3402/jev.v2i0.20360

538 23. Smith JA, Daniel R (2016) Human vaginal fluid contains exosomes that have an inhibitory
539 effect on an early step of the HIV-1 life cycle. AIDS. doi:
540 10.1097/QAD.0000000000001236

541 24. Muth DC, McAlexander MA, Ostrenga LJ, et al (2015) Potential role of cervicovaginal
542 extracellular particles in diagnosis of endometriosis. BMC Vet Res 11:187. doi:
543 10.1186/s12917-015-0513-7

544 25. Sergeeva AM, Pinzon Restrepo N, Seitz H (2013) Quantitative aspects of RNA silencing
545 in metazoans. Biochem 78:613–626. doi: 10.1134/S0006297913060072BCM78060795
546 [pii]

547 26. Bartel DP (2009) MicroRNAs: target recognition and regulatory functions. Cell 136:215–
548 233. doi: S0092-8674(09)00008-7 [pii]10.1016/j.cell.2009.01.002

549 27. Turchinovich A, Weiz L, Langheinz A, Burwinkel B (2011) Characterization of
550 extracellular circulating microRNA. Nucleic Acids Res 39:7223–7233. doi: gkr254
551 [pii]10.1093/nar/gkr254

552 28. Arroyo JD, Chevillet JR, Kroh EM, et al (2011) Argonaute2 complexes carry a population
553 of circulating microRNAs independent of vesicles in human plasma. Proc Natl Acad Sci U
554 S A 108:5003–5008. doi: 1019055108 [pii]10.1073/pnas.1019055108

555 29. Witwer KW, Sarbanes SL, Liu J, Clements JE (2011) A plasma microRNA signature of
556 acute lentiviral infection: biomarkers of CNS disease. AIDS 204:1104–1114. doi:
557 10.1097/QAD.0b013e32834b95bf

558 30. Zubakov D, Boersma AW, Choi Y, et al (2010) MicroRNA markers for forensic body
559 fluid identification obtained from microarray screening and quantitative RT-PCR
560 confirmation. Int J Leg Med 124:217–226. doi: 10.1007/s00414-009-0402-3

561 31. Seashols-Williams S, Lewis C, Calloway C, et al (2016) High-throughput miRNA
562 sequencing and identification of biomarkers for forensically relevant biological fluids.
563 Electrophoresis. doi: 10.1002/elps.201600258

564 32. Muth DC, McAlexander MA, Ostrenga LJ, et al (2015) Potential role of cervicovaginal
565 extracellular particles in diagnosis of endometriosis. Bmc Vet Res. doi: 10.1186/s12917-
566 015-0513-7

567 33. Thery C, Amigorena S, Raposo G, Clayton A (2006) Isolation and characterization of
568 exosomes from cell culture supernatants and biological fluids. Curr Protoc Cell Biol
569 Chapter 3:Unit 3 22. doi: 10.1002/0471143030.cb0322s30

570 34. McAlexander MA, Phillips MJ, Witwer KW (2013) Comparison of methods for miRNA
571 extraction from plasma and quantitative recovery of RNA from cerebrospinal fluid. Front
572 Genet 4:83. doi: 10.3389/fgene.2013.00083

573 35. Chen C, Ridzon DA, Broomer AJ, et al (2005) Real-time quantification of microRNAs by
574 stem-loop RT-PCR. Nucleic Acids Res 33:e179. doi: 33/20/e179 [pii]10.1093/nar/gni178

575 36. Witwer KW, Sarbanes SL, Liu J, Clements JE (2011) A plasma microRNA signature of
576 acute lentiviral infection: biomarkers of central nervous system disease. AIDS 25:2057–
577 2067. doi: 10.1097/QAD.0b013e32834b95bf

578 37. Clough E, Barrett T (2016) The Gene Expression Omnibus Database. Methods Mol Biol

1418:93–110. doi: 10.1007/978-1-4939-3578-9_5

38. Lotvall J, Hill AF, Hochberg F, et al (2014) Minimal experimental requirements for definition of extracellular vesicles and their functions: a position statement from the International Society for Extracellular Vesicles. J Extracell Vesicles 3:26913. doi: 10.3402/jev.v3.26913

39. Witwer KW, Soekmadji C, Hill AF, et al (2017) Updating the MISEV minimal requirements for extracellular vesicle studies: building bridges to reproducibility. J Extracell Vesicles. doi: 10.1080/20013078.2017.1396823

40. Van Deun J, Mestdagh P, Agostinis P, et al (2017) EV-TRACK: transparent reporting and centralizing knowledge in extracellular vesicle research. Nat Methods 14:228–232. doi: 10.1038/nmeth.4185

41. Nguyen HPT, Simpson RJ, Salamonsen LA, Greening DW (2016) Extracellular Vesicles in the Intrauterine Environment: Challenges and Potential Functions. Biol Reprod 95:109–109. doi: 10.1095/biolreprod.116.143503

42. Campoy I, Lanau L, Altadill T, et al (2016) Exosome-like vesicles in uterine aspirates: a comparison of ultracentrifugation-based isolation protocols. J Transl Med 14:180. doi: 10.1186/s12967-016-0935-4

43. Zegels G, Aa G, Raemdonck V, et al (2009) Comprehensive proteomic analysis of human cervical-vaginal fluid using colposcopy samples. Proteome Sci. doi: 10.1186/1477-5956-7-17

44. Gravett MG, Thomas A, Schneider KA, et al PROTEOMIC ANALYSIS OF CERVICAL-

VAGINAL FLUID: IDENTIFICATION OF NOVEL BIOMARKERS FOR DETECTION OF INTRA-AMNIOTIC INFECTION. doi: 10.1021/pr060149v

45. Arroyo JD, Chevillet JR, Kroh EM, et al (2011) Argonaute2 complexes carry a population of circulating microRNAs independent of vesicles in human plasma. Proc Natl Acad Sci U S A 108:5003–8. doi: 10.1073/pnas.1019055108

46. Pritchard CC, Kroh E, Wood B, et al (2012) Blood cell origin of circulating microRNAs: a cautionary note for cancer biomarker studies. Cancer Prev Res 5:492–497. doi: 1940-6207.CAPR-11-0370 [pii]10.1158/1940-6207.CAPR-11-0370

47. Akhter A, Patel JL, Farooq F, et al De Novo Acute Myeloid Leukemia in Adults: Suppression of MicroRNA-223 is Independent of LMO2 Protein Expression BUT Associate With Adverse Cytogenetic Profile and Undifferentiated Blast Morphology. Appl Immunohistochem Mol Morphol 23:733–9. doi: 10.1097/PAI.0000000000000145

48. Tombak A, Ay OI, Erdal ME, et al (2015) MicroRNA Expression Analysis in Patients with Primary Myelofibrosis, Polycythemia vera and Essential Thrombocythemia. Indian J Hematol Blood Transfus 31:416–25. doi: 10.1007/s12288-014-0492-z

49. Giray BG, Emekdas G, Tezcan S, et al (2014) Profiles of serum microRNAs; miR-125b-5p and miR223-3p serve as novel biomarkers for HBV-positive hepatocellular carcinoma. Mol Biol Rep 41:4513–9. doi: 10.1007/s11033-014-3322-3

50. Bertoli G, Cava C, Castiglioni I (2015) MicroRNAs: New Biomarkers for Diagnosis, Prognosis, Therapy Prediction and Therapeutic Tools for Breast Cancer. Theranostics 5:1122–43. doi: 10.7150/thno.11543

621 51. Wang S, Zhang R, Claret FX, Yang H (2014) Involvement of microRNA-24 and DNA
622 methylation in resistance of nasopharyngeal carcinoma to ionizing radiation. Mol Cancer
623 Ther 13:3163–74. doi: 10.1158/1535-7163.MCT-14-0317

624 52. Li J, Hu L, Tian C, et al (2015) microRNA-150 promotes cervical cancer cell growth and
625 survival by targeting FOXO4. BMC Mol Biol 16:24. doi: 10.1186/s12867-015-0052-6

626 53. Huang J, Wang F, Argyris E, et al (2007) Cellular microRNAs contribute to HIV-1
627 latency in resting primary CD4+ T lymphocytes. Nat Med 13:1241–1247. doi: nm1639
628 [pii]10.1038/nm1639

629 54. Swaminathan S, Murray DD, Kelleher AD (2013) miRNAs and HIV: unforeseen
630 determinants of host-pathogen interaction. Immunol Rev 254:265–280. doi:
631 10.1111/imr.12077

632 55. Sisk JM, Witwer KW, Tarwater PM, Clements JE (2013) SIV replication is directly
633 downregulated by four antiviral miRNAs. Retrovirology 10:95. doi: 1742-4690-10-95
634 [pii]10.1186/1742-4690-10-95

635 56. Wang X, Ye L, Zhou Y, et al (2011) Inhibition of anti-HIV microRNA expression: a
636 mechanism for opioid-mediated enhancement of HIV infection of monocytes. Am J Pathol
637 178:41–47. doi: S0002-9440(10)00089-1 [pii]10.1016/j.ajpath.2010.11.042

638 57. Swaminathan S, Suzuki K, Seddiki N, et al (2012) Differential regulation of the Let-7
639 family of microRNAs in CD4+ T cells alters IL-10 expression. J Immunol 188:6238–6246.
640 doi: jimmunol.1101196 [pii]10.4049/jimmunol.1101196

641 58. Klase Z, Kale P, Winograd R, et al (2007) HIV-1 TAR element is processed by Dicer to

642 yield a viral micro-RNA involved in chromatin remodeling of the viral LTR. BMC Mol
643 Biol 8:63. doi: 1471-2199-8-63 [pii]10.1186/1471-2199-8-63

644 59. Wagschal A, Rousset E, Basavarajaiah P, et al (2012) Microprocessor, Setx, Xrn2, and
645 Rrp6 co-operate to induce premature termination of transcription by RNAPII. Cell
646 150:1147–1157. doi: 10.1016/j.cell.2012.08.004S0092-8674(12)00999-3 [pii]

647 60. Whisnant AW, Bogerd HP, Flores O, et al (2013) In-Depth Analysis of the Interaction of
648 HIV-1 with Cellular microRNA Biogenesis and Effector Mechanisms. MBio. doi:
649 10.1128/mBio.00193-13e00193-13 [pii]mBio.00193-13 [pii]

650 61. Sung TL, Rice AP (2009) miR-198 inhibits HIV-1 gene expression and replication in
651 monocytes and its mechanism of action appears to involve repression of cyclin T1. PLoS
652 Pathog 5:e1000263. doi: 10.1371/journal.ppat.1000263

653 62. Gardiner C, Vizio D Di, Sahoo S, et al (2016) Techniques used for the isolation and
654 characterization of extracellular vesicles: results of a worldwide survey. J Extracell
655 Vesicles. doi: 10.3402/jev.v5.32945

656 63. Witwer KW, Halushka MK (2016) Towards the Promise of microRNAs - Enhancing
657 reproducibility and rigor in microRNA research. RNA Biol 0. doi:
658 10.1080/15476286.2016.1236172

659 64. La Rocca G, Olejniczak SH, Gonzalez AJ, et al (2015) In vivo, Argonaute-bound
660 microRNAs exist predominantly in a reservoir of low molecular weight complexes not
661 associated with mRNA. Proc Natl Acad Sci U S A 112:767–772. doi:
662 10.1073/pnas.1424217112

663 **FIGURE LEGENDS**

664 **Figure 1. EVs are found in cervicovaginal lavage. A)** Particle concentrations of CVL 100,000
665 × *g* ultracentrifuge (UC) pellets (blue) monitored weekly over five weeks for two SIV-negative
666 ("control") and four SIV-infected subjects. Red arrows indicate estimated ovulation for SIV-
667 negative subjects. **B and C)** Transmission electron micrographs of CVL 10,000 × *g* pellet **(B)**
668 and 100,000× *g* pellet **(C)** confirm presence of bacteria and EVs (B) and EV-like particles (C).
669 Western blot: enrichment of CD63 and CD81 markers **(D)** and absence of ER marker calnexin
670 **(E)** in pooled 10,000 and 10,000 × *g* pellet fractions. Vaginal tissue homogenate and dendritic
671 cell 100,000 × *g* pellet controls were also positive for CD63 and CD81. EV luminal markers
672 syntenin and TSG101 were present in cellular but not putative EV samples.

673

674 **Figure 2. miRNA profile of CVL fractions.** Targeted miRNA profiles were determined by
675 custom TaqMan low-density array (TLDA). Hierarchical clustering of samples and features
676 (Pearson correlation, average linkage) of data: raw **(A)** or normalized by **(B)** quantiles or **(C)** a
677 geometric mean approach as described in the methods. Abundance scale: red (high) to low (blue).

678

679 **Figure 3: Relative abundance of miRNAs in centrifuged CVL fractions. A)** Abundant
680 miRNAs in descending order based on Cq values normalized to the geometric mean for each
681 sample. Inset: average of all miRNAs in UC pellet and UC supernatant. Error bars: SEM. **B)**
682 miRNAs in each fraction (10,000× g pellet=p10, 110,000 × g pellet=p100, 110,000× g
683 supernatant=S100) are significantly correlated ($p<0.0001$, Spearman). **C)** miRNA expression in

684 EV-enriched fractions (p10, p100) as a percentage of total estimated expression
685 (p10+p100+S100 by Cq) in ascending order, from miR-27a-3p (7.9%) to miR-28-3p (32.0%).

686

687 **Figure 4. miRNA qPCR validation. A)** Stem-loop reverse transcription/qPCR validation of UC
688 p100 samples, all subjects and time points (individual dots). **B)** Ranks of abundant miRNAs
689 based on qPCR and TLDA Cq data.

690

691 **Figure 5**. **miR-186-5p downregulation: SIV. A)** By TLDA, miRs-186, -222, and -200c were
692 significantly less abundant in the CVL p100 fraction of infected subjects, ** p□<□0.01, ***
693 p<0.001. **B)** By qPCR, miRs-186, -375, and -125b were significantly less abundant, **
694 p□<□0.01, *** p<0.001.

695

696 **Figure 6: miRNA-186-5p inhibits p24 release.** Monocyte-derived macrophages from human
697 donors were infected with HIV-1 BaL. **A)** p24 production increased >2 fold for all donors from 3
698 to 9 days post-infection (dpi), infected but otherwise untreated cells. **B-D)** Transfection of miR-
699 186 mimic was associated with a decrease of p24 release compared with untransfected controls
700 (NC) and control RNA mimic-transfected controls (RC); ns=not significant, * p<0.05, ** p<0.01,
701 **** p<0.0001 (ANOVA followed by Bonferroni correction for multiple tests). Results were
702 obtained from 8 to 11 replicate experiments with cells from 3 human donors.

703

Figure 7: miRNA-186-5p mimic transfection inconsistently suppresses HIV-1 gag mRNA production. Apparent downregulation of gag mRNA (qPCR assay with standard curve) was observed in miR-186-transfected monocyte-derived macrophages from only 1 of 3 donors compared with control RNA-transfected cells (RC). Overall, results were insignificant by t-test, $p>0.1$, with multiple replicates of cells from 3 human donors.

A

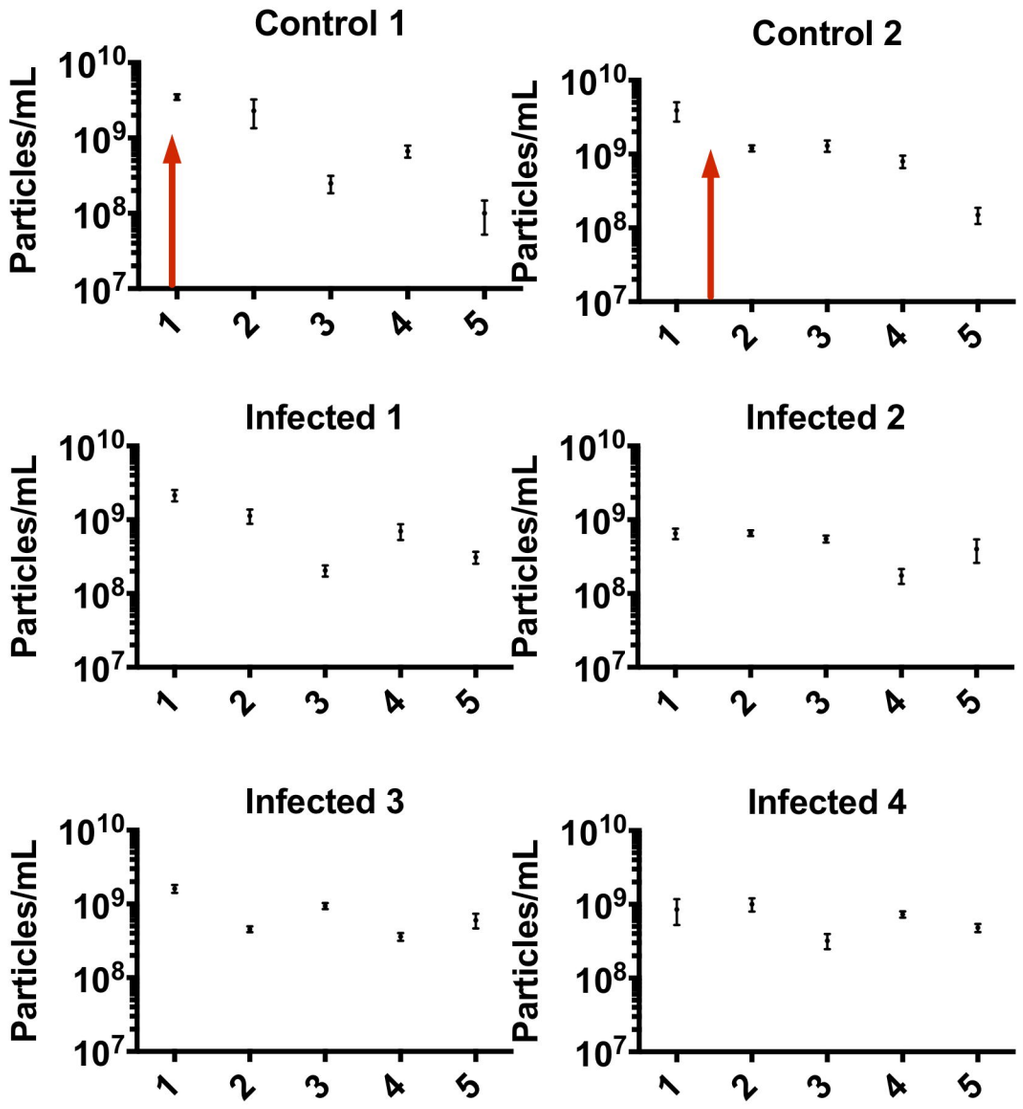
Control 1
Control 2
Infected 1
Infected 2
Infected 3
Infected 4
Particles/mL
10^{10}
10^{9}
10^{8}
10^{7}
1
2
3
4
5

B

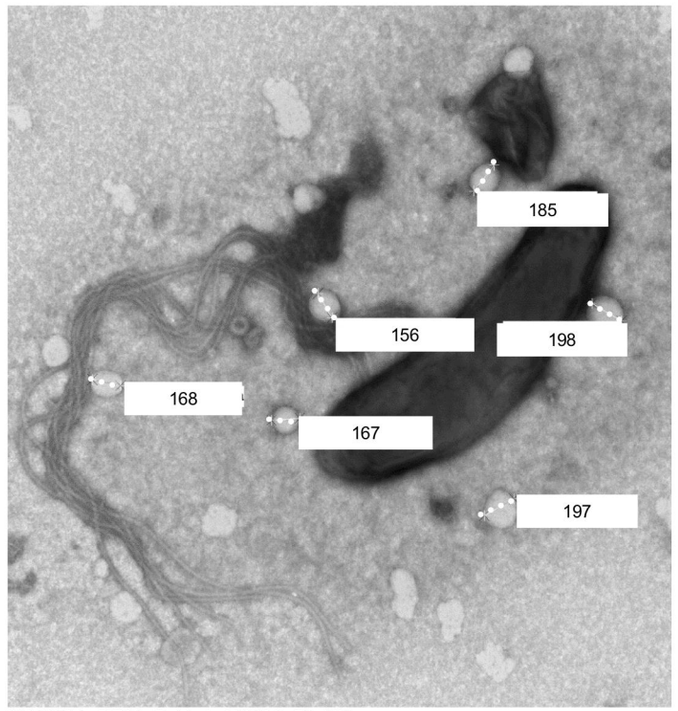
185
156
198
168
167
197
20150714_CVL1k Pellet_130718_B7_005
Cal: 0.001871 um/pix
4:30:08 PM 7/14/2015
500 nm
HV=80.0kV
Direct Mag: 40000x

C

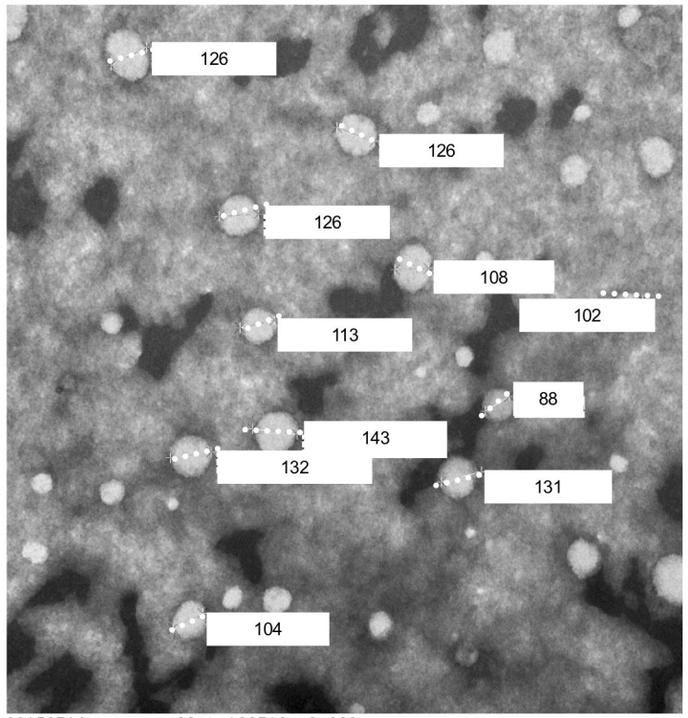
126
126
126
108
102
113
88
143
132
131
104
20150714_CVLUC Pellet_130718_B8_009
Cal: 0.001036 um/pix
4:49:06 PM 7/14/2015
500 nm
HV=80.0kV
Direct Mag: 70000x

D

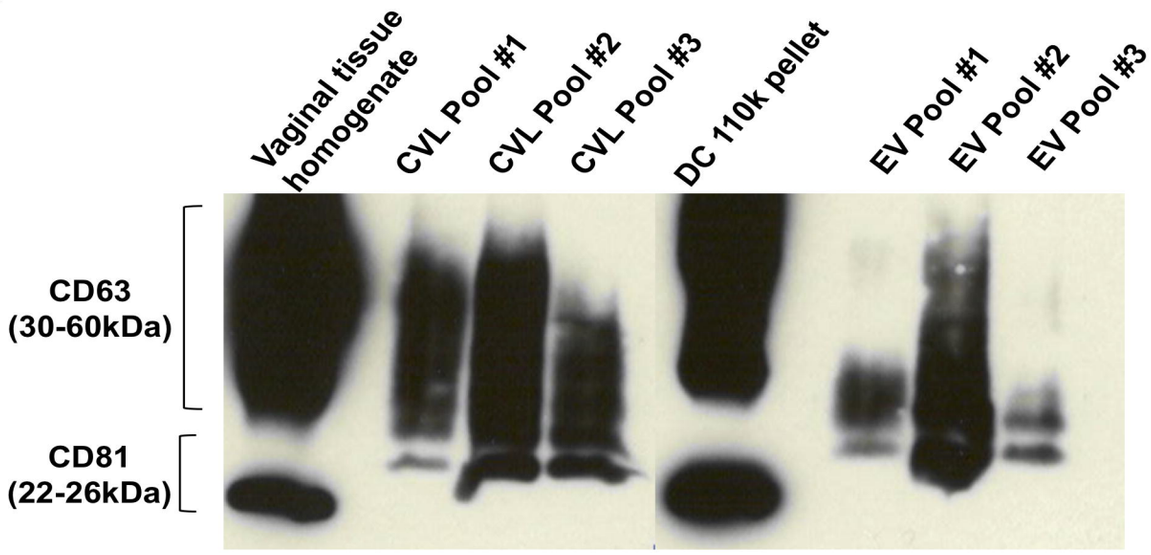
Vaginal tissue homogenate
CVL Pool #1
CVL Pool #2
CVL Pool #3
DC 110k pellet
EV Pool #1
EV Pool #2
EV Pool #3
CD63 (30-60kDa)
CD81 (22-26kDa)

E

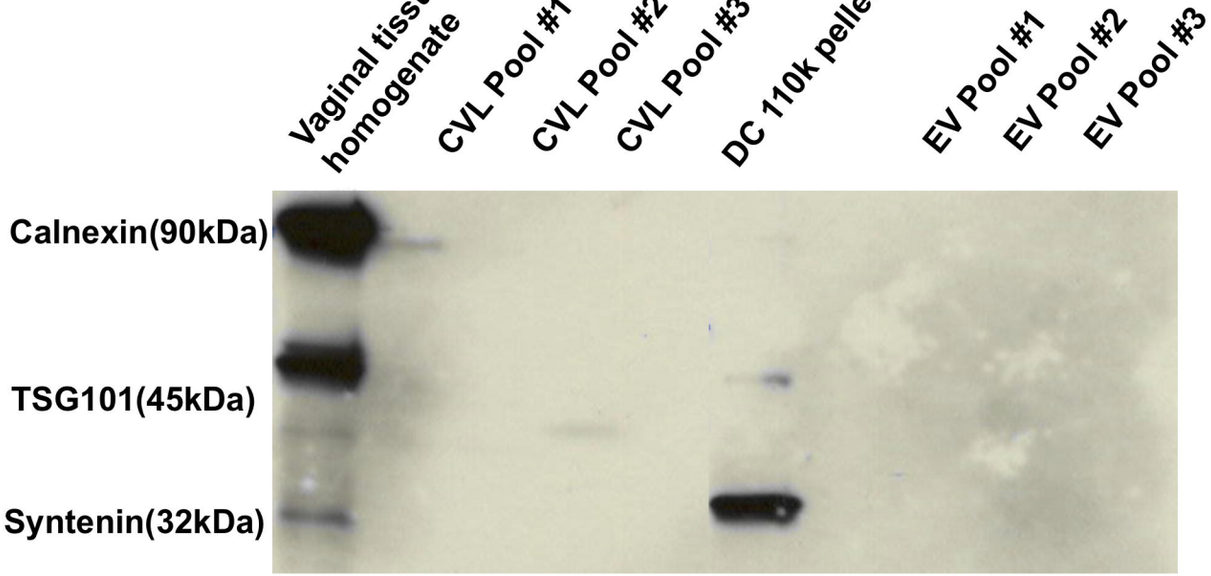
Vaginal tissue homogenate
CVL Pool #1
CVL Pool #2
CVL Pool #3
DC 110k pellet
EV Pool #1
EV Pool #2
EV Pool #3
Calnexin(90kDa)
TSG101(45kDa)
Syntenin(32kDa)

A

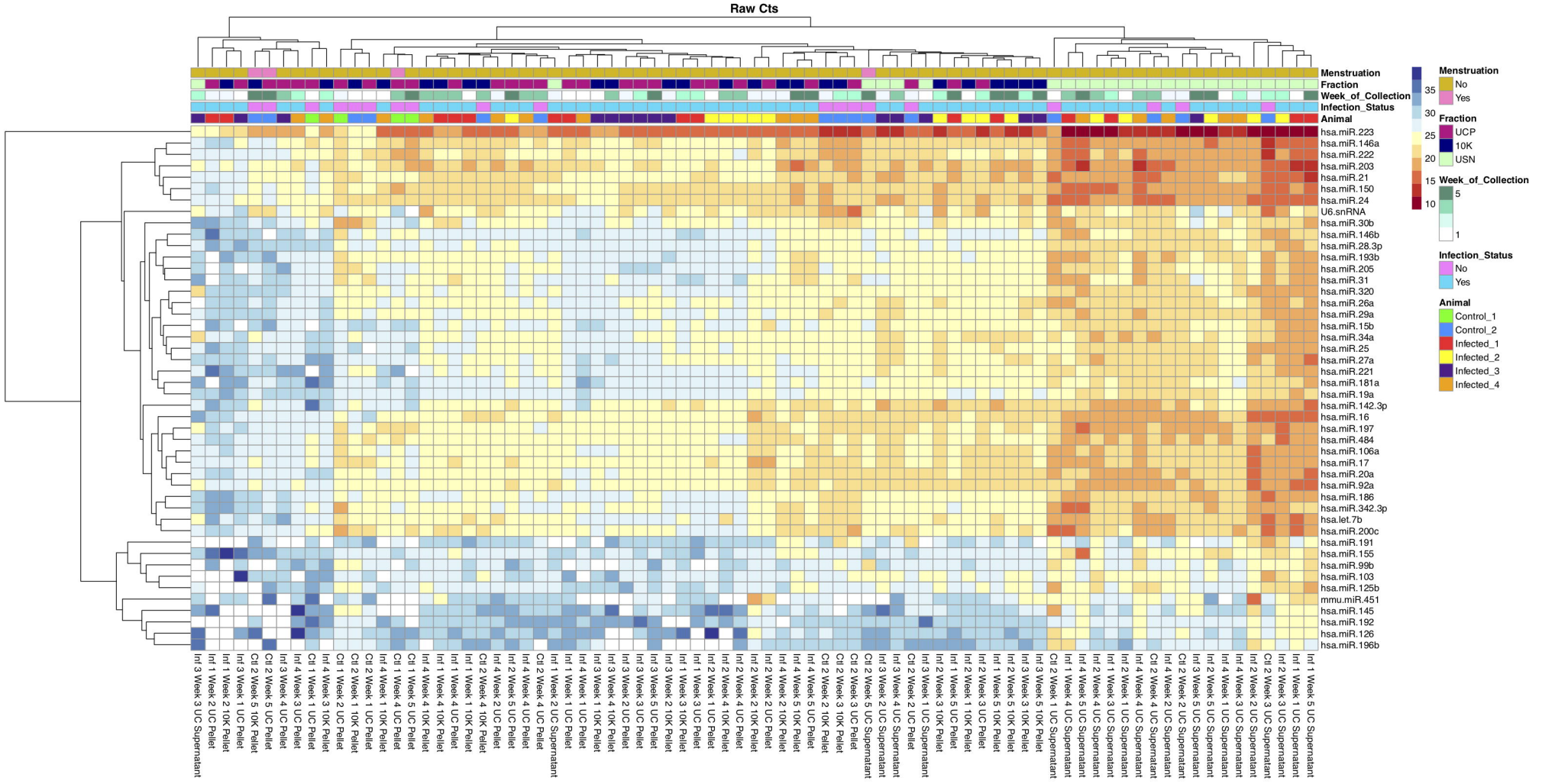

B

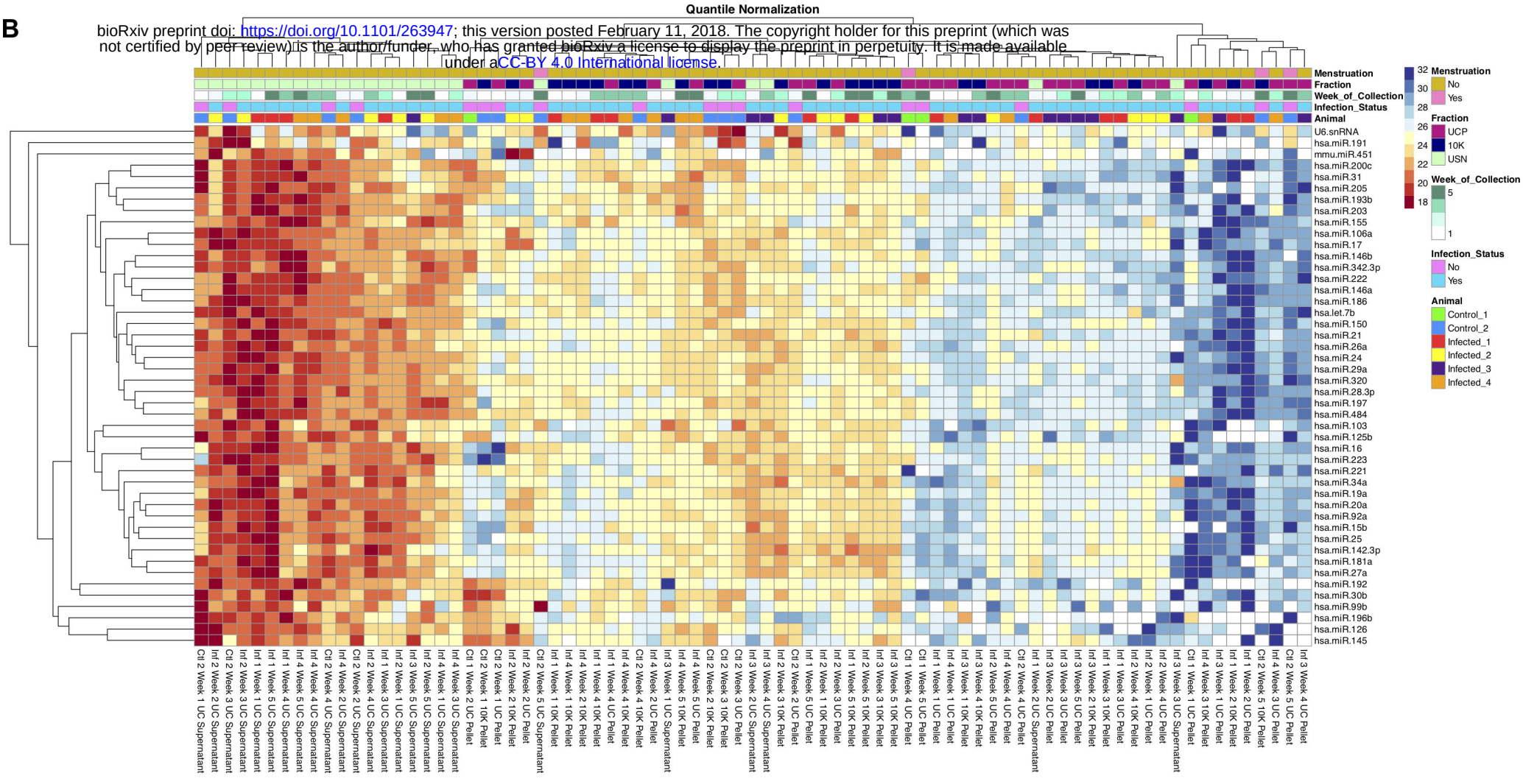

C

A

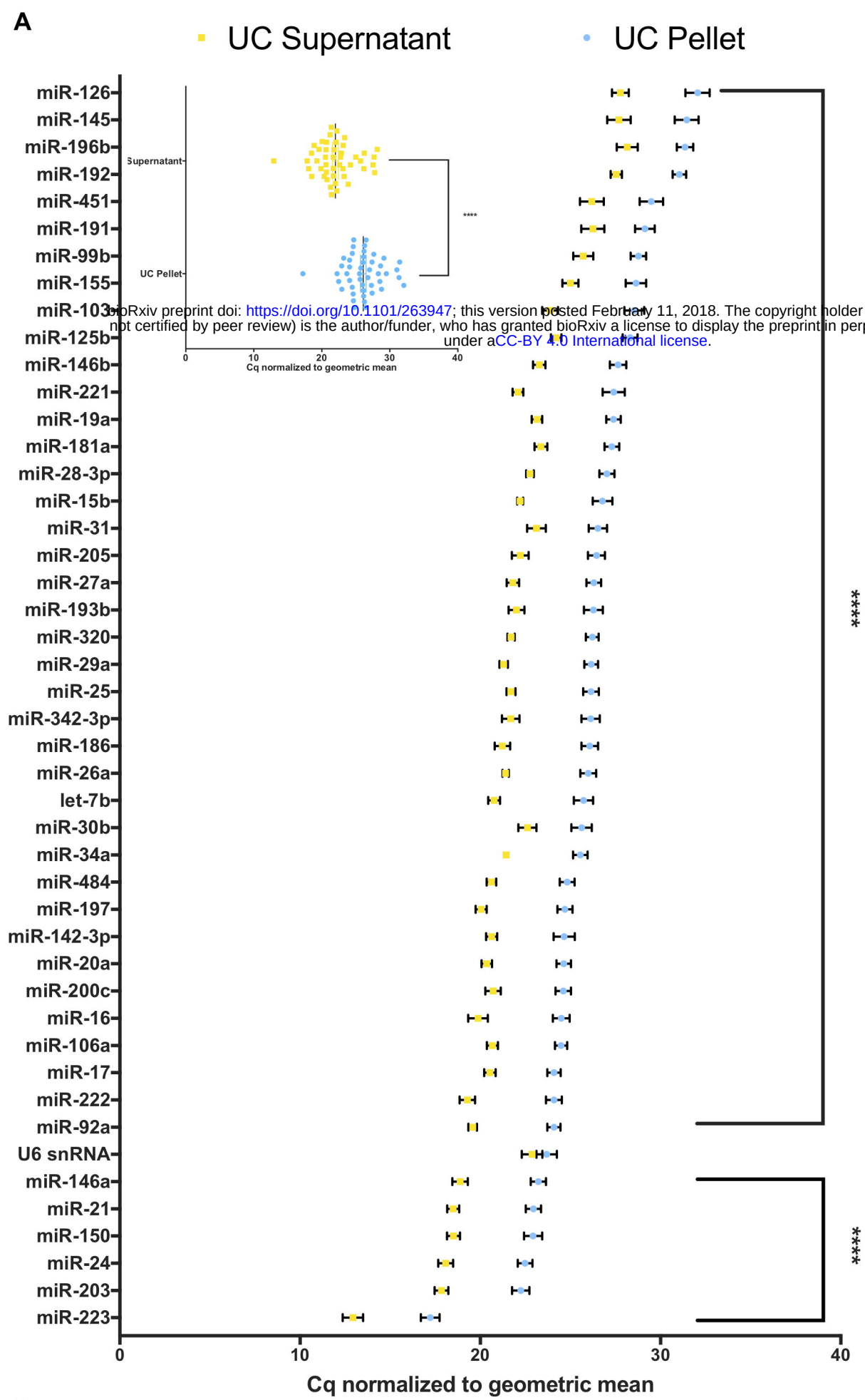

C

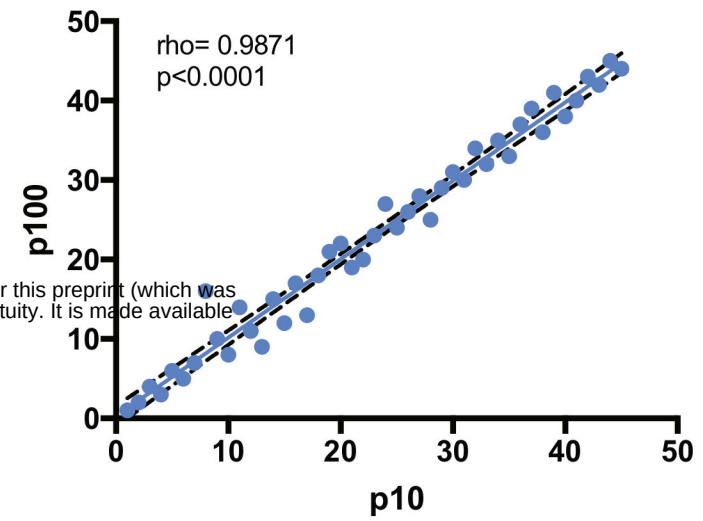

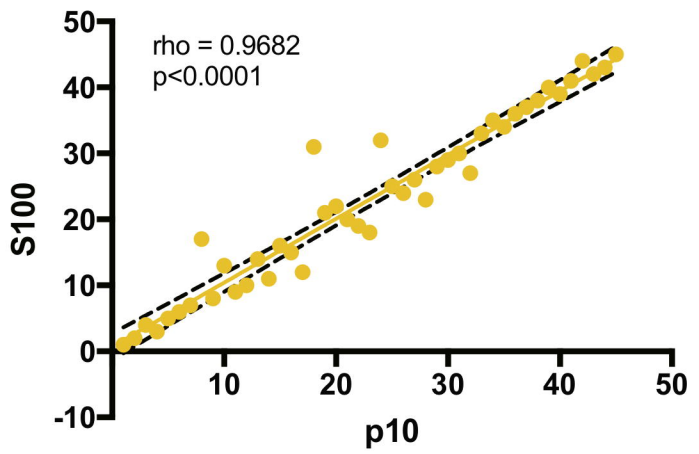

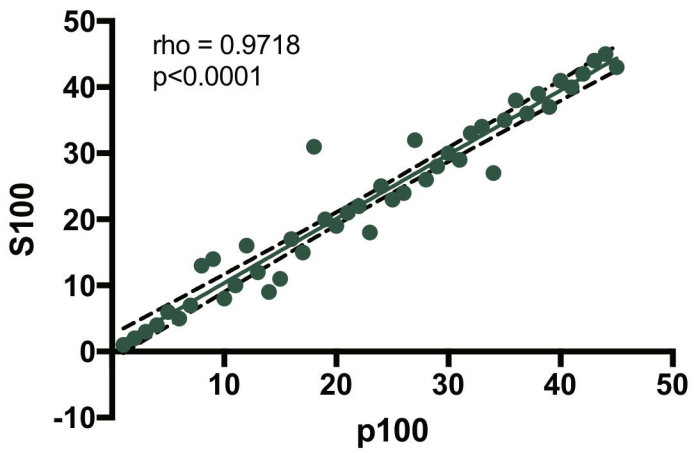

B

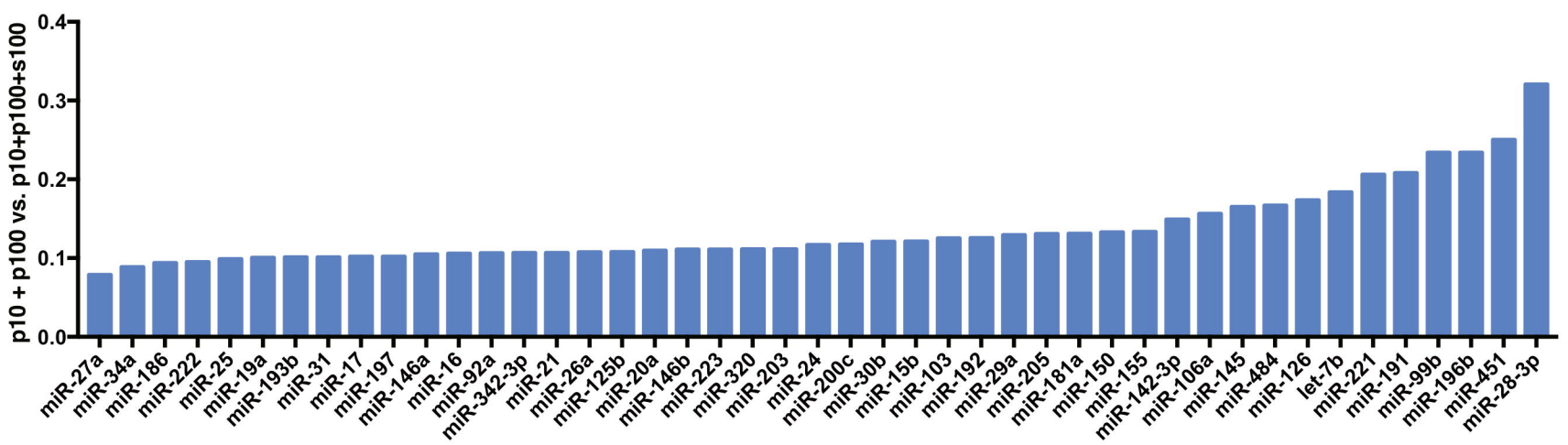

A

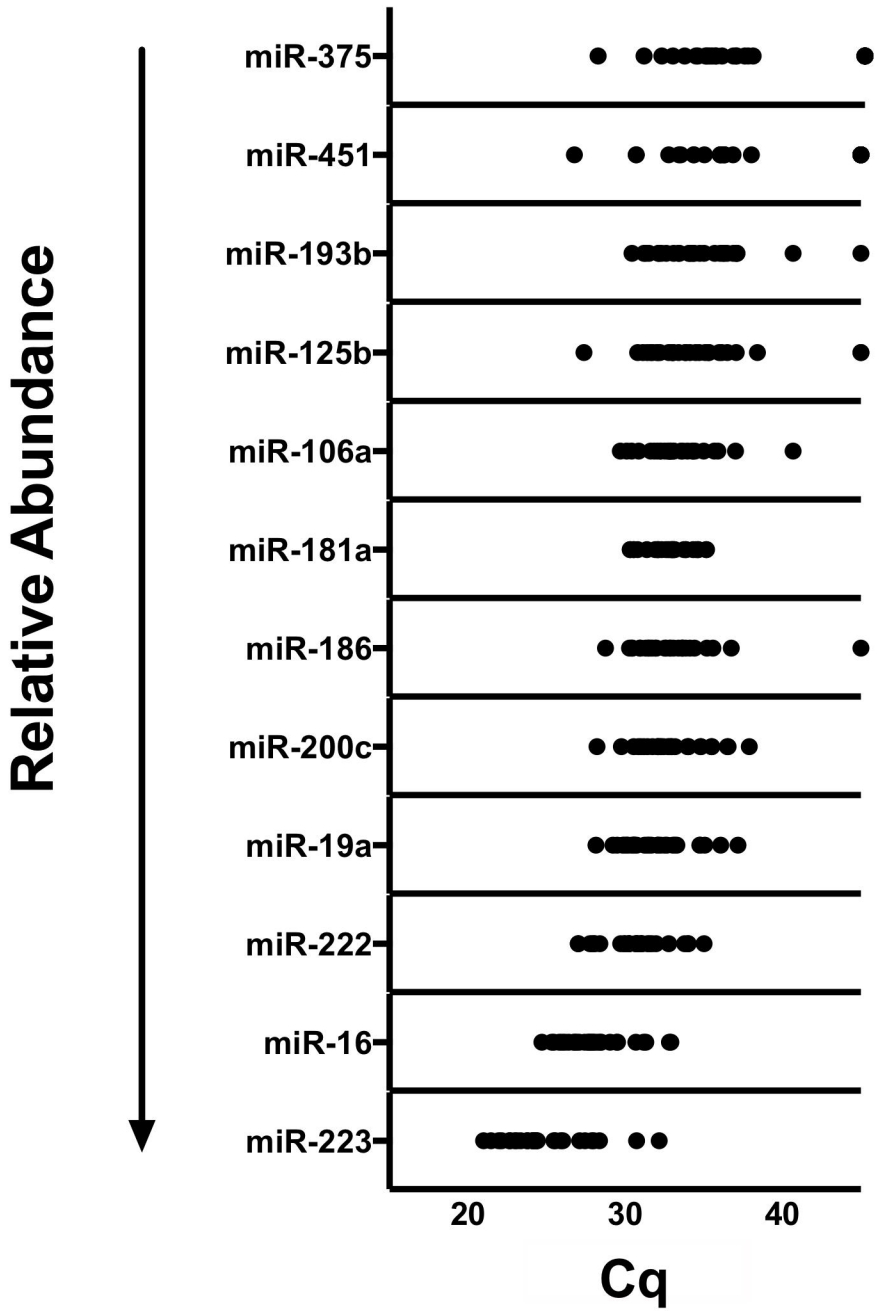

B

Rank (qPCR)	miRNA	Rank (TLDA)
1	miR-223-3p	1
2	miR-16-5p	3
3	miR-222-3p	2
4	miR-19a-3p	9
5	miR-200c-3p	4
6	miR-186-5p	6
7	miR-181a-5p	8
8	miR-106a-5p	5
9	miR-125b-5p	10
10	miR-193b-3p	7
11	miR-451a-5p	11

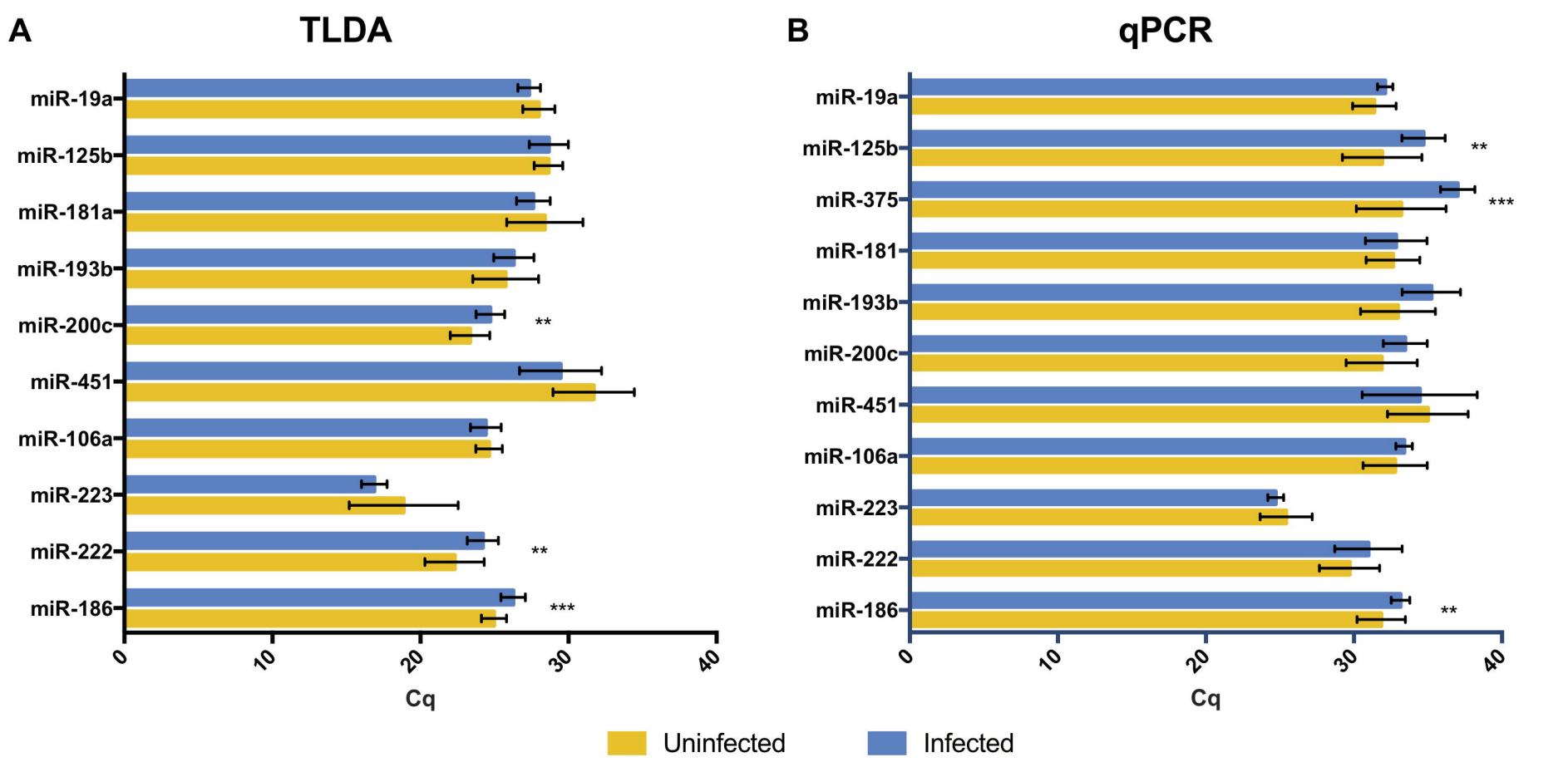
A
TLDA
miR-19a
miR-125b
miR-181a
miR-193b
miR-200c
miR-451
miR-106a
miR-223
miR-222
miR-186
**
**
***
0
10
20
30
40
Cq
B
qPCR
miR-19a
miR-125b
miR-375
miR-181
miR-193b
miR-200c
miR-451
miR-106a
miR-223
miR-222
miR-186
**
***
**
0
10
20
30
40
Cq
Uninfected
Infected

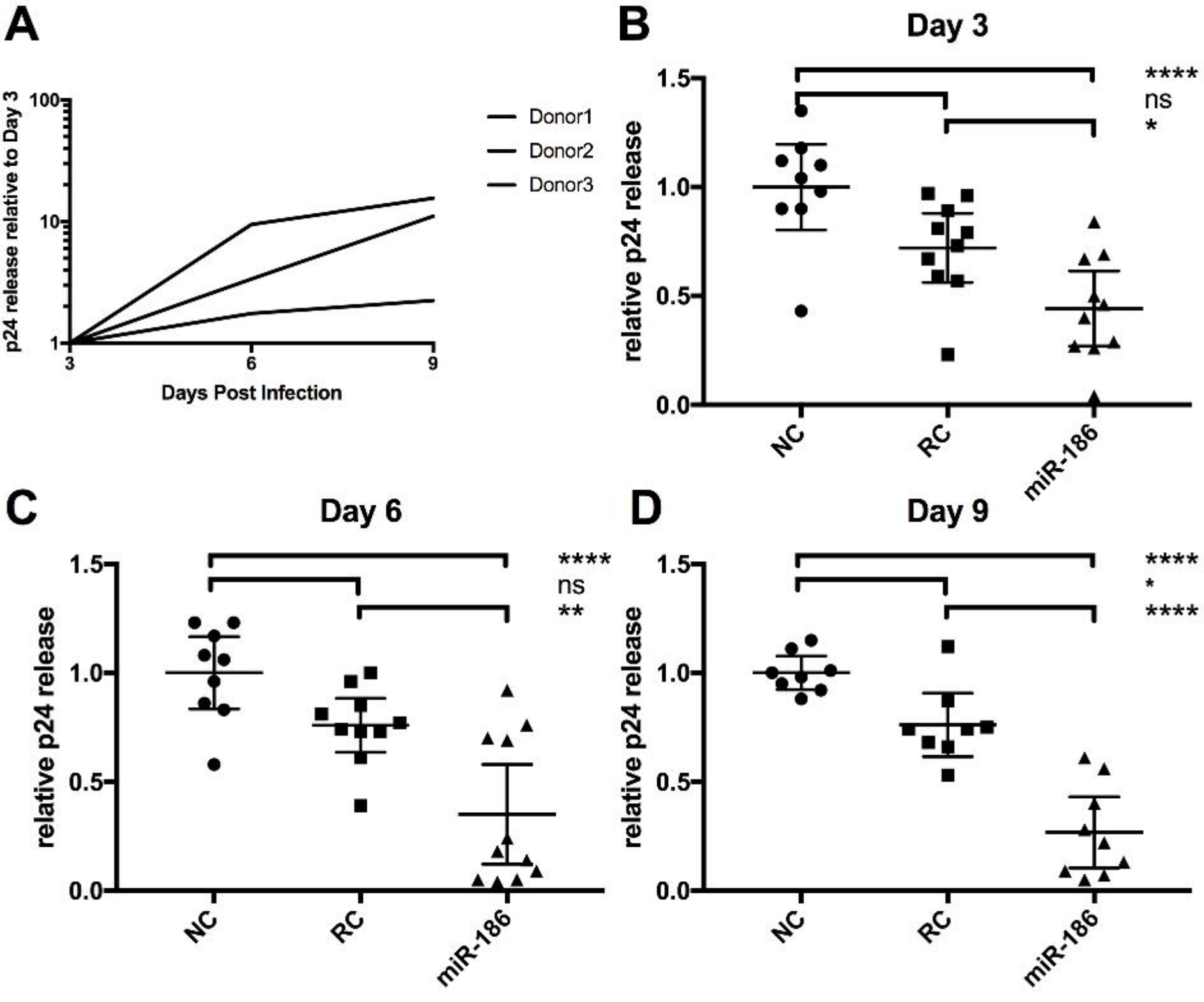
A
p24 release relative to Day 3
100
10
1
3
6
9
Days Post Infection
Donor1
Donor2
Donor3
B
Day 3
relative p24 release
1.5
1.0
0.5
0.0
****
ns
*
NC
RC
miR-186
C
Day 6
relative p24 release
1.5
1.0
0.5
0.0
****
ns
**
NC
RC
miR-186
D
Day 9
relative p24 release
1.5
1.0
0.5
0.0
****
*
****
NC
RC
miR-186

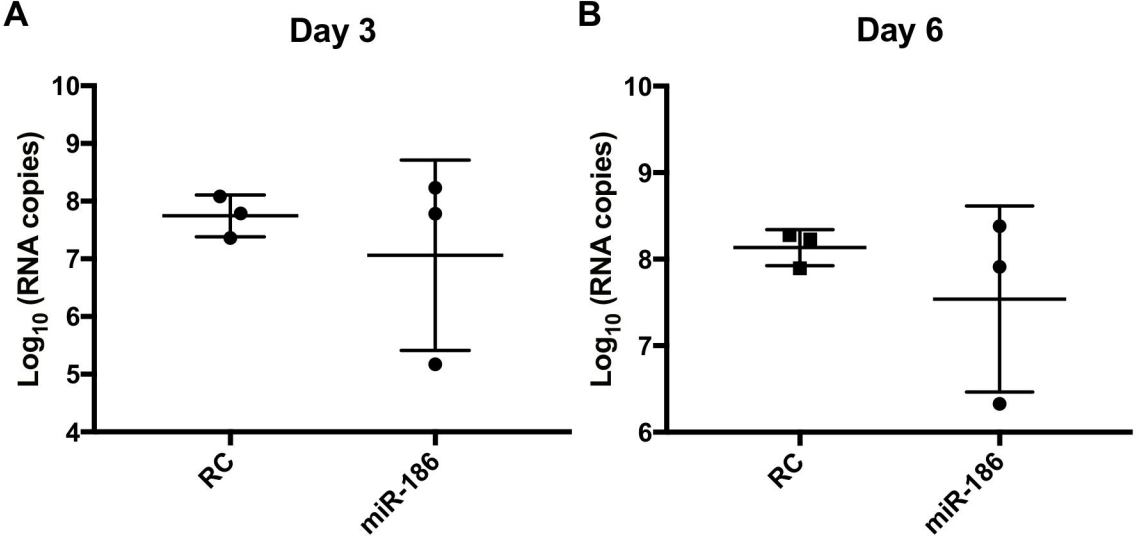
A
Day 3
Log10 (RNA copies)
10
9
8
7
6
5
4
RC
miR-186
B
Day 6
Log10 (RNA copies)
10
9
8
7
6
RC
miR-186